



Determination of Henry's law constant and the diffusion and polytropic coefficients of air in aviation fuel

Patrick F. Dunn*, Flint O. Thomas, James B. Leighton, Dayu Lv

Department of Aerospace and Mechanical Engineering, University of Notre Dame, Notre Dame, IN 46556, United States

ARTICLE INFO

Article history:

Received 19 May 2010

Received in revised form 24 November 2010

Accepted 26 November 2010

Available online 10 December 2010

Keywords:

Aviation fuel

Polytropic constant

Diffusion coefficient

Henry's law constant

Bubble

ABSTRACT

The volume change of air microbubbles on surface nucleation sites was studied experimentally and compared with predictions. Measurements were used to determine the polytropic constant, the diffusion coefficient, and the Henry's law constant of air in distilled water, dodecane, and JP-8 aviation fuel. The liquids were exposed to sub-atmospheric pressures, but above their vapor pressures. In one type of experiment, bubble size reduction was recorded as the liquid's ambient pressure was increased from a low pressure to atmospheric pressure through a series of step increases. The results were used to determine the polytropic constant. In another type of experiment, bubble growth was monitored in time following a sudden reduction in the liquid's pressure from ambient. The Epstein–Plesset model of mass diffusion was coupled with a Lipschitzian optimization technique to determine the values of the diffusion coefficient and Henry's law constant.

© 2010 Elsevier Ltd. All rights reserved.

1. Introduction

This paper presents the results of an investigation to determine the polytropic constant, the diffusion coefficient, and Henry's law constant for air in JP-8 aviation fuel. The study was undertaken because of a lack of this information in the open literature. Such property information is a necessary part of the larger effort to understand cavitation behavior in modern aircraft-fuel systems [1].

Cavitation in an aircraft-fuel system can lead to unexpected degradation in system performance and/or damage to fuel system components. These systems often are characterized by complex internal flow geometries that involve very narrow flow path restrictions and sharp turns. Such geometries can lead to localized regions of high fluid velocity and low static pressure. For some scenarios in which the static pressure is close to but above the liquid vapor pressure, gaseous cavitation occurs. For other scenarios, the static pressure can go below the liquid vapor pressure, leading to both gaseous and vaporous cavitation. The present study focused on bubble growth related to gaseous cavitation.

It is well known that nucleation sites on surfaces are necessary to catalyze the bubble growth that produces cavitation. The nucleation of bubbles into gaseous or vaporous cavities have been classified into four different types of events [2]. Two types of nucle-

ation events can occur in flow devices such as in aircraft-fuel systems at pressures *at or above* the vapor pressure of the liquid. This is attributed to pre-existing gas and/or vapor-containing sites, which primarily are stable on the solid surfaces that confine the liquid or are present within the liquid (microparticles) [3]. Solid microparticles in the form of silicates and iron oxides typically are present in aviation fuel and harbor numerous nucleation sites for cavitation inception. In addition, fuel containment surfaces can have many nucleation sites.

JP-8 is the aviation fuel used most commonly by the United States military [4]. Approximately 60 billion gallons of JP-8 and its commercial equivalent, Jet A-1, are used annually worldwide [5]. JP-8 is a complex mixture of over 228 hydrocarbons and various additives to meet military specification MIL-DTL-83133 [6,7]. It is comprised of 18% (by volume) aromatics, 20% naphthenes, 60% parafins, 2% olefins [8]. The primary constituent of JP-8 is kerosene, which consists of hydrocarbons, mainly in the C₉–C₁₆ range [9]. Details regarding the bulk fluid properties and the chemical composition of JP-8 can be found in [7].

Modelling the flow of JP-8 through complex geometries requires accurate knowledge of the properties of air dissolved in JP-8. Little such information is available in the open literature for the properties that govern polytropic and diffusional processes. These include the polytropic constant, the diffusion coefficient, and Henry's law constant. Further, there is no information in the open literature about the effect of sub-atmospheric pressure on these three properties. Addressing this paucity of information through benchmark experiments was the primary reason for the present investigation.

* Corresponding author. Tel.: +1 574 631 6089.

E-mail address: pdunn@nd.edu (P.F. Dunn).

2. Experimental approach

Two different series of experiments were performed using the same experimental apparatus and diagnostics. These characterized the volumetric change of air microbubbles on surface nucleation sites immersed in a static, constant-temperature liquid. The liquid was exposed to sub-atmospheric pressures, but above its vapor pressure. In the first series, the relatively ‘instantaneous’ volumetric change was recorded as the liquid’s ambient pressure was increased from a low pressure to atmospheric pressure through a series of step increases. This determined the microbubble’s pV^k (pressure–volume) behavior, as characterized by its polytropic constant, k . In the second series, the microbubble’s longer-term (diffusional) growth was monitored in time following a sudden reduction in the liquid’s ambient pressure. This information was used to determine values of the diffusion coefficient, D , and Henry’s law constant, H . Similar techniques have been employed in the past to determine the diffusion coefficients for a gas in a liquid, such as O_2 , N_2 , and He in water and in organic liquids [10].

A schematic is shown in Fig. 1. Further details of the experimental apparatus and diagnostics used for the present experiments are described [11]. The test cell, mounted on a three-axis micro-traverse, consisted of a hollow steel cube (~ 5 cm-length side) with six circular ports used for either viewing windows or instrument feed-through. The bottom port held a pedestal that extended into the near center of the cell. Three side ports were used for windows to view the interior of the test cell. The fourth side port was used as a feed-through for a type-K thermocouple that monitored the liquid temperature. The top port supported an adapter that connected the test cell to a vacuum system.

The test cell was illuminated using two fiber-optic light guides (positioned at each of the side-port windows) connected to a halogen lamp. A CCD camera with a macro lens and $6\times$ extension tube was used to monitor the microbubble’s volume change. This magnification produced a resolution of $3.7\ \mu\text{m}$ (a zero-order uncertainty for a length measurement of $\pm 1.9\ \mu\text{m}$ at the 95% confidence level [12]). The camera’s framing rate was 33 Hz. The output of the camera was recorded by a personal computer. Individual frames of the captured video subsequently were analyzed using MATLAB[®].

A pressure transducer was used to measure the static pressure within the test cell. A ball valve isolated the test cell from a 3.8-L reservoir. This reservoir was maintained at a desired pressure (to as low as 0.5 psia for up to 2 h with only a 0.02 psia decrease in pressure). The overall uncertainty in the measured pressure was

$\pm 0.25\ \text{kPa}$ ($\pm 0.04\ \text{psi}$), estimated at the 95% confidence level. The liquid temperature was monitored and remained at $295 \pm 1\ \text{K}$ during all experiments.

The top surface of a stainless steel pedestal contained the microbubble nucleation site. This was a 1 mm-deep hole drilled into the surface with 319 μm -diameter drill bit. This is shown schematically in Fig. 2.

Three fluids were used: aviation fuel (JP-8), dodecane ($C_{12}H_{26}$), and distilled water. Dodecane served as a single-component hydrocarbon surrogate of JP-8, being its largest mass fraction component ($\sim 23\%$) and having a well defined vapor pressure. Distilled water was used to validate the experimental technique and to provide a baseline for comparison with the other fluids.

The properties of the three fluids used are summarized in Table 1. It is important to note that the property values of JP-8 can differ because of the variability in its mixture, as well as its storage history and location. For example, the vapor pressure of JP-8 gathered from seven different locations in the US ranged from 74 Pa to 430 Pa (at 294 K [70 °F]), with an average vapor pressure of 240 Pa [14]. The static pressures used in the present investigation were above this range of JP-8’s vapor pressures and those of dodecane and water.

JP-8 in its natural, unsettled state contains solid microparticles in the form of iron oxides and silicates. Data provided by the Honeywell Corporation indicated a particle mass concentration of $\sim 2\ \text{mg/L}$ fuel and a number concentration of $\sim 10^7$ particles/L fuel. Each of the liquids used in the present experiments was essentially free of particles. The distilled/deionized water was obtained from a filtered laboratory water-purification system. The dodecane was purchased commercially in 5-L containers. While the JP-8 did contain microparticles, as described previously, these were effectively filtered from the JP-8 over time by gravitational settling in the storage tanks.

In the present experiments, JP-8 was stored at ambient temperature and pressure ($\sim 295\ \text{K}$ and $\sim 101.3\ \text{kPa}$, respectively) in closed, 3.8-L containers until an experiment was performed. Under these ambient conditions, the dissolved content of air in JP-8 is $0.139\ \text{mm}^3\ \text{air/mm}^3\ \text{fuel}$ (based upon 78% of N_2 and 21% O_2 , having solubilities of $0.120\ \text{mm}^3\ N_2/\text{mm}^3\ \text{fuel}$ and $0.215\ \text{mm}^3\ O_2/\text{mm}^3\ \text{fuel}$, respectively) [7]. The fuel was obtained commercially and was not degassed prior to experiment. This was done to examine the behavior of JP-8 stored under typical conditions without any special treatment or handling such that the results were more relevant for typical situations.

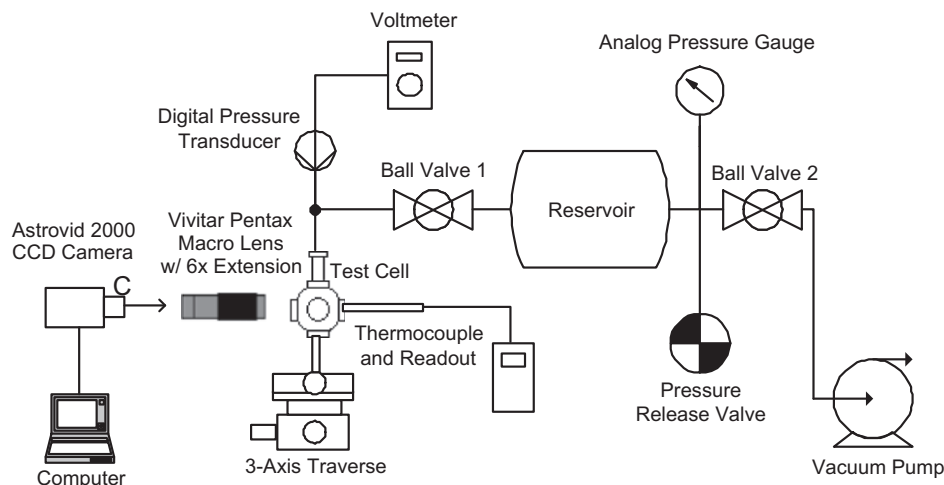


Fig. 1. Schematic of the experimental apparatus.

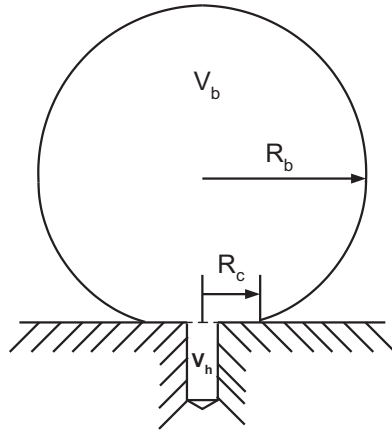


Fig. 2. Schematic of a bubble and its drilled nucleation site.

Table 1
Properties of fluids used in the experiments. Values obtained from [13–15].

	Water	C ₁₂ H ₂₆	JP-8
Molecular weight, <i>MW</i> (g/mol)	18.015	170.34	173
Density, ρ (kg/m ³)	997	752	796
Absolute viscosity, μ (mPa s)	0.99	1.34	1.62
Surface tension, σ (mN/m)	72	25	23
Vapor pressure, p_v (Pa)	2123	16	240

3. Results

For both series of experiments described in the following, a change in microbubble volume occurs as a result of an imposed change in liquid pressure. The pressure of the gas inside the microbubble, $p_g(t)$, is given by

$$p_g(t) = p_l(t) - p_v + 2\sigma/R(t), \tag{1}$$

where $p_l(t)$ is the liquid pressure, p_v the vapor pressure of the liquid, σ is the surface tension of the liquid, and $R(t)$ is the radius of the microbubble. The term $2\sigma/R(t)$ represents the change in pressure

that occurs across the microbubble–liquid interface. In the first series, the microbubble radius is measured before and after a step increase in pressure, both at steady state. In the second series, the microbubble radius is measured over the time following a step decrease in pressure.

For all three liquids examined in these experiments, the liquid pressure, either before or after the imposed change in pressure, was on the order of 10–1000× greater than the liquid vapor pressure and the interface pressure change. Thus, for these experiments, $p_g(t) - p_l(t)$ and the microbubble’s content is primarily air. For this situation, the change in the microbubble volume is governed by the mass diffusion of primarily air (mainly N₂ and O₂).

3.1. First experimental series

In this series of experiments, the microbubble’s radius was recorded as the liquid’s ambient pressure was increased from a low pressure to atmospheric pressure though a series of step increases in pressure. For the range of pressures and times investigated, microbubbles of air in either water, dodecane or JP-8 were found to respond nearly instantaneously (< 1 ms) and isothermally to step changes in pressure.

The experimental results are presented in Figs. 3–5 for water, dodecane and JP-8, respectively. In these figures, the dimensionless volume, V^* , is plotted versus dimensionless pressure (the pressure ratio), p^* . In this manner, the polytropic relation becomes $kV^* = p^*$. These dimensionless variables are defined as

$$V^* = \log_{10}[V_i/V_f] \tag{2}$$

and

$$p^* = -\log_{10}[p_{g_i}/p_{g_f}]. \tag{3}$$

Here, V is the entire volume of the gas microbubble ($V_g + V_h$), where V_g is the volume of the microbubble *per se* and V_h is the constant volume of the nucleation site hole (refer to Fig. 2). The subscripts i and f denote initial and final steady-state values, respectively. In each case, the solid line depicts the least-squares linear regression fits of the data and the dashed lines indicate the lower and upper 95% confidence interval limits.

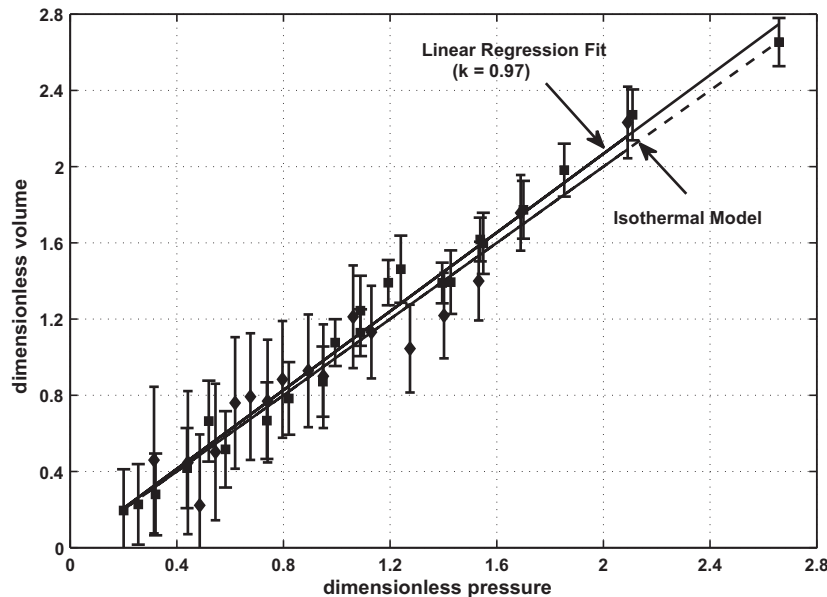


Fig. 3. Dimensionless volume versus dimensionless pressure for water. The solid line is the linear best-fit of the 39 data pairs; the dashed lines are the lower and upper 95% confidence limits. The regression coefficient is 0.9826 for 39 data values.

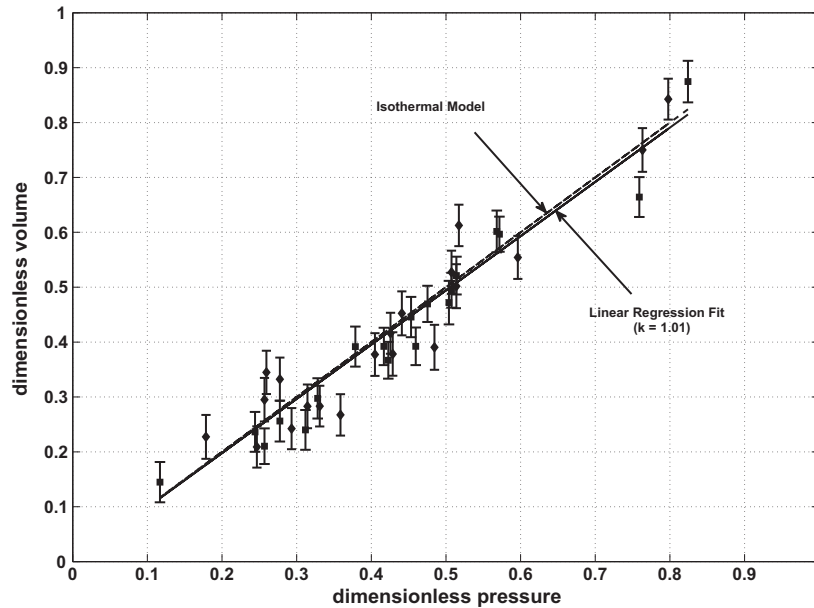


Fig. 4. Dimensionless volume versus dimensionless pressure for dodecane. The solid line is the linear best-fit of the 39 data pairs; the dashed lines are the lower and upper 95% confidence limits. The regression coefficient is 0.9624 for 39 data values.

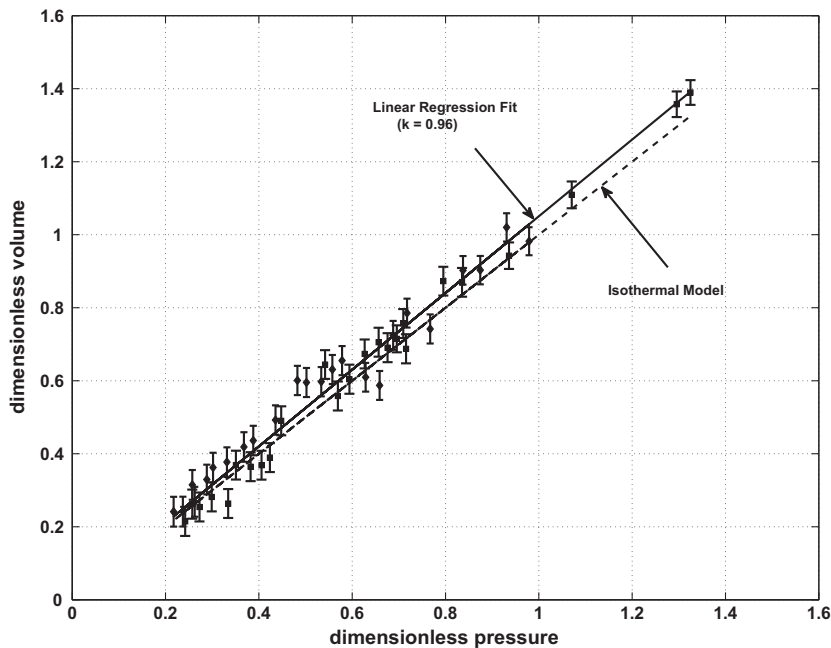


Fig. 5. Dimensionless volume versus dimensionless pressure for JP-8. The solid line is the linear best-fit of the 49 data pairs; the dashed lines are the lower and upper 95% confidence limits. The regression coefficient is 0.9887 for 49 data values.

For all three liquids, the slope, k , is unity to within experimental uncertainty (water: 0.967; dodecane: 1.012; JP-8: 0.952). Further, the confidence that the data are described by a linear fit is greater than 99% (see [12]). For water, the slope agrees with that reported by Ran and Katz [16] to within 0.004, or 0.4%. These results imply that the response of an air bubble to a sudden pressure change is isothermal in each liquid, for which k is unity.

3.2. Second experimental series

In this series of experiments, the microbubble's growth was monitored following a sudden reduction in the liquid's pressure

from ambient to a sub-atmospheric value. The resulting measured microbubble radius versus time for each of the three liquids at various pressures are presented in Figs. 6–8. For each liquid and pressure case, the microbubble radius increased with time. As the liquid pressure was reduced, the microbubble radius became relatively larger and its growth rate greater as compared the previous higher-pressure case. This data was compared with the predictions of the Epstein–Plesset model [17], which are shown as solid curves in the figures.

The Epstein–Plesset model considers the diffusion of a gas bubble in a liquid–gas solution. It considers the change of the radius of a center-stationary, spherical bubble in time for either under-satu-

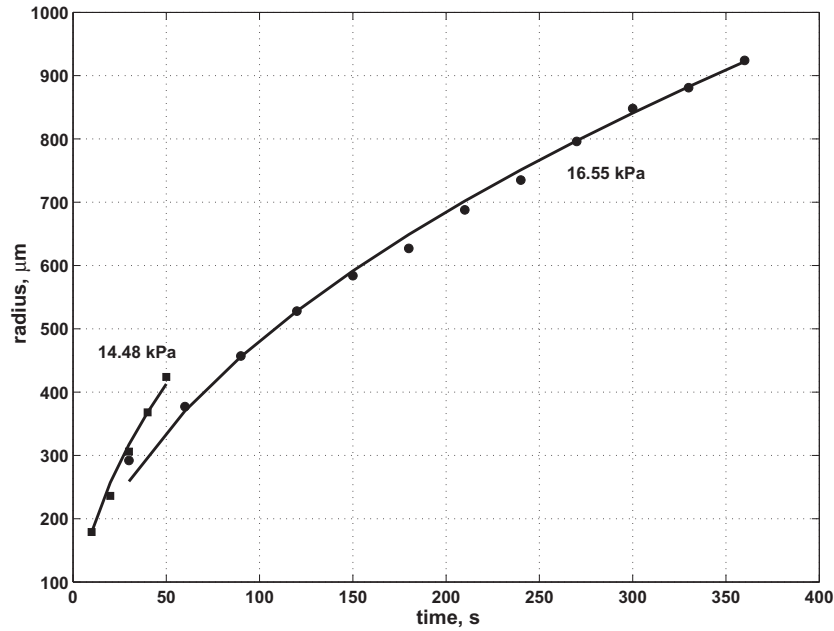


Fig. 6. Bubble radius versus time for two different-pressure water cases. Solid curve depicts model; solid circles data.

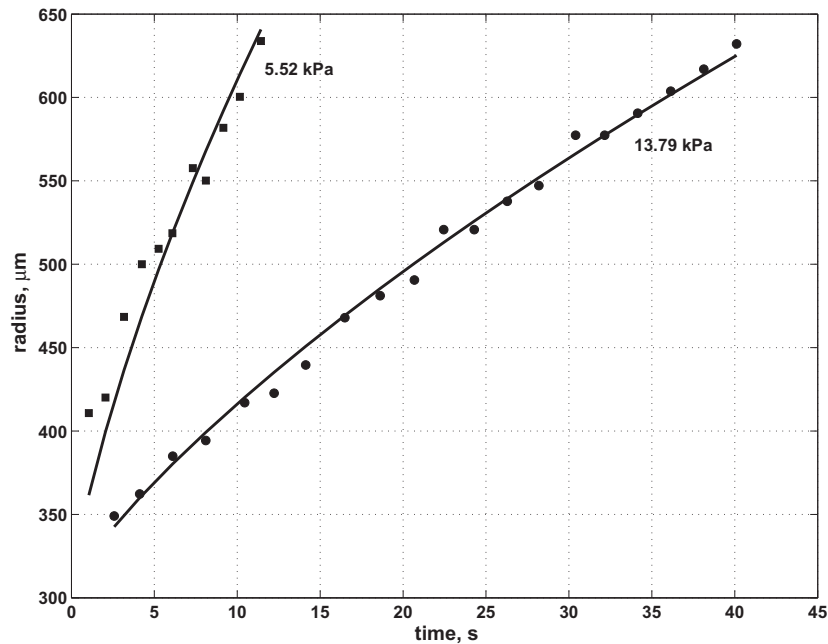


Fig. 7. Bubble radius versus time for two different-pressure dodecane cases. Solid curve depicts model; solid circles data.

rated or over-saturated liquid–gas solutions. The time rate of change of the bubble radius, dR/dt , results from diffusional mass transfer and can be expressed as

$$\frac{dR}{dt} = \frac{D}{H} \left[\frac{(p_i - p)(R_u T / MW)}{p + 2\sigma/R} \right] \left[\frac{1}{R} + \frac{1}{\sqrt{\pi D t}} \right] \left[1 - \left(\frac{R_0}{\sqrt{2}R} \right)^2 \right], \quad (4)$$

in which $R = R(t)$ is the radius, R_0 the initial radius, R_u the universal gas constant equal to 8313.3 J/(kg mole K), MW the molecular weight (=28.966 kg/kg mole for air), T the temperature, p_i the initial pressure of the liquid, p the pressure of the saturated liquid, D the diffusion coefficient of the gas in the liquid, and H Henry's law constant for the gas.

The last term in brackets on the right hand side of Eq. (4) is a present modification to the original equation to account for the reduced surface area of the bubble being in contact with a solid surface. The actual surface area of the bubble in contact with the liquid, A_b , equals the surface area of a bubble of radius R minus that of a truncated spherical cap of radius R_c (refer to Fig. 2). This difference can be nondimensionalized by the surface area of a bubble to become $\chi = 1 - (R_c/\sqrt{2}R)^2$. In the experiments, χ was initially ~ 0.5 . As time progressed, χ rapidly approached unity, reaching a value of 0.93 at $R = 10R_c$.

Using the initial condition $R(0) = R_0$, which is determined experimentally, Eq. (4) can be integrated numerically using a 4th-order Runge–Kutta technique to find $R(t)$. For the present situation, this

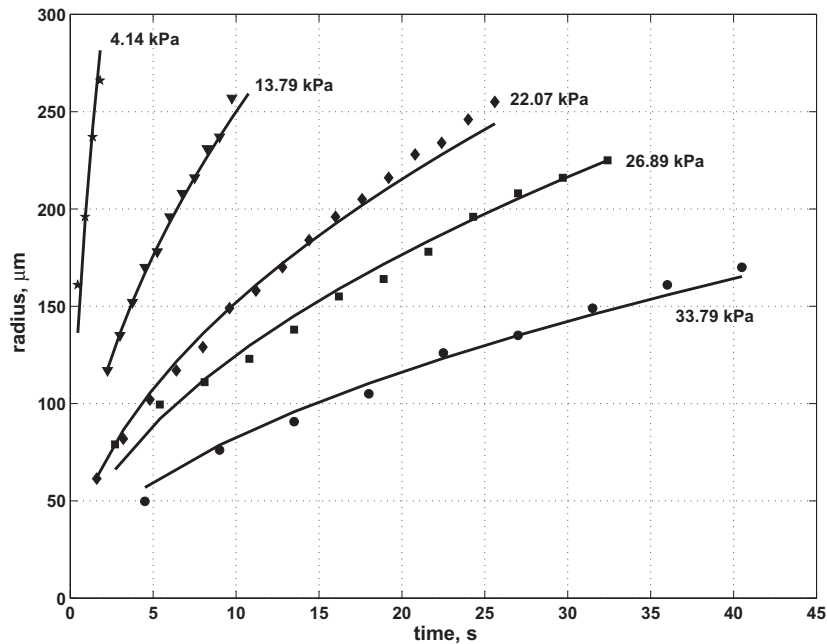


Fig. 8. Bubble radius versus time for five different-pressure JP-8 cases. Solid curve depicts model; solid circles data.

approach was coupled with an optimization technique to find the values of D and H that gave the best-fit with data. The deterministic optimal search method called DIRECT [18,19], was implemented to find global optimum values. One of its advantages is the ability of search globally in a multi-dimension parameters space with simple boundaries.

The numerical search was conducted in two steps. First, D and H were allowed to vary. The initial radius of the bubble was assumed to be of the order of that observed in the experiments (typically several micrometers). This initial residual-minimization search yielded values of H that were close to the known or estimated values presented in Table 2. The search supported that H did not depend upon the pressure, as is known for pressures up to approx 5 atm [20]. The converged values of D , however, were found to vary with pressure. In the second, subsequent step, H was held fixed for each liquid. Values of D for each liquid were found to increase with decreasing pressure. The final, optimum values of H and D for all experimental cases are presented in Table 3.

The resulting pressure-diffusion coefficient pair values could be fitted best by the relation $pD = \text{constant}$. This relation is similar to that obtained for a binary mixture of gases [20,21]. A comparison

Table 3

Determined values of H and D . Units are kPa for pressure, $\text{MPa m}^3/\text{kg}$ for H , and $(\text{m}^2/\text{s}) \times 10^9$ for D . Subscript m for H and D denotes values obtained from minimization search.

Fluid	Pressure	H_m	D_m
JP-8	33.79	4.80	7.5
JP-8	26.89	4.80	12.7
JP-8	22.07	4.80	13.6
JP-8	13.79	4.80	19.5
JP-8	4.14	4.80	40.2
Dodecane	13.79	4.40	20.8
Dodecane	5.52	4.40	33.1
Water	14.48	4.70	13.2
Water	16.55	4.70	8.4

of this pD relation with the optimum values of H and D and data is shown in Fig. 9 with pressure as a parameter for the five JP-8 pressure cases examined. Similar results were obtained for the dodecane and water cases. The values of D for all five JP-8 cases agree with the $pD = \text{constant}$ relation to within $\pm 30\%$ (at 95% confidence).

Extrapolation of the $pD = \text{constant}$ relation to atmospheric conditions, as shown in Fig. 9 for the JP-8 cases, yielded values of the diffusion coefficient at standard atmospheric conditions of $2.63 \times 10^{-9} \text{ m}^2/\text{s}$, $2.32 \times 10^{-9} \text{ m}^2/\text{s}$, and $1.63 \times 10^{-9} \text{ m}^2/\text{s}$, for air into JP-8, dodecane, and water, respectively. Previously obtained values at atmospheric conditions for air into water (stationary bubble diffusion) range from approximately $1.6 \times 10^{-9} \text{ m}^2/\text{s}$ [26] to $4.7 \times 10^{-9} \text{ m}^2/\text{s}$ [24]. Also, a value of $2.5 \times 10^{-9} \text{ m}^2/\text{s}$ at 293 K was reported for air into water [27]. The relatively lower value of D obtained in the present experiments can be explained by “the effect on diffusion of a plane surface tangent to a sphere” [26] (refer to Fig. 2), which reduces the diffusivity by a factor of $\ln 2$ ($=0.69$). The values of D for dodecane and JP-8 are within the ranges of the estimated reference values (see Table 2). The values of H for all three liquids also are very close to those estimated. The overall uncertainties, estimated at the 95% confidence level, are $\pm 5\%$ for H and $\pm 10\%$ for D . Note that the only published values listed in Table 2 were those of D and H for air in water and H for air in dodecane.

Table 2

Reference values for H and D . Units are kPa for pressure, $\text{MPa m}^3/\text{kg}$ for H_{cr} , and $(\text{m}^2/\text{s}) \times 10^9$ for D_{cr} . Values are for atmospheric pressure. Subscript cr for H and D denotes values obtained computation and/or published reference. Superscripts denote sources for values:

Liquid	H_{cr}	D_{cr}
JP-8	4.34 ^a	0.87–2.50 ^b
Dodecane	4.33 ^c	1.20–3.50 ^b
Water	3.97–5.90 ^d	2.10–4.73 ^d ; 2.03 ^e ; 1.6–3.0 ^f

^a Upper limit from [22].

^b Using Stokes–Einstein diffusion equation and range of D values for water from 1.63 to 4.73.

^c Average of five values from [23].

^d From [24] from 17 °C to 47.3 °C.

^e From [25].

^f From [26] for stationary bubble from 8 °C to 27 °C.

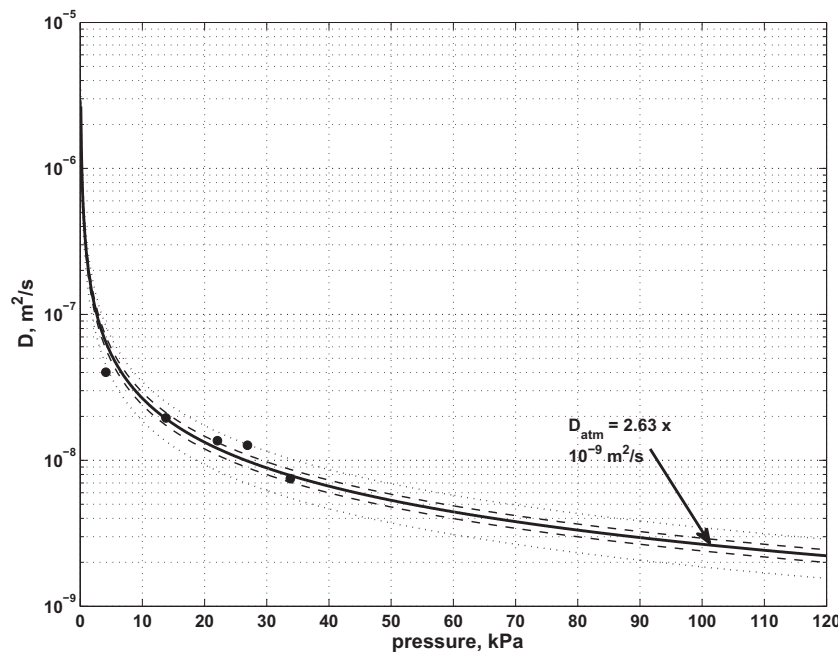


Fig. 9. Diffusion coefficient versus pressure for five JP-8 cases. Solid curve depicts $Dp_{\infty} = \text{constant}$ best-fit; solid circles optimized data values. The dashed and dotted curves are $\pm 10\%$ and $\pm 30\%$ deviations from the solid curve, respectively.

4. Summary and conclusions

Values of the polytropic constant, the diffusion coefficient, and Henry's law constant for air in JP-8, dodecane and water were determined through combined experimental and numerical-optimization approach. The values obtained for water were consistent with published reference values. Those for dodecane and JP-8 were similar to estimated values.

The polytropic constant of air in either JP-8, dodecane or water was found to be unity. This implies that the volume change of air microbubbles in solution can be modelled as an isothermal process. Henry's law constant was found to be independent of pressure and different for all three liquids. The diffusion coefficient was determined to increase with decreasing pressure for air in each of the three liquids and described by the relation $pD = \text{constant}$ for each liquid. This behavior is similar to that found for a mixture of binary gases in which the diffusion coefficient is inversely proportional to the pressure.

These findings, which are summarized in Table 3, provide much needed property information for air in JP-8. They can be used in the modelling of flow through geometries representative of aircraft-fuel systems.

Acknowledgements

The experimental results presented in this paper were part of the MS thesis research of J. Leighton. D. Lv performed the optimization calculations. This research was supported by the Honeywell Corporation. We especially thank Steve Emo, Corey Bourassa, and Abigail Parsons for their many technical interactions and support throughout this research.

References

- [1] Dunn PF, Thomas FO, Davis MP, Dorofeeva IE. Experimental characterization of aviation-fuel cavitation. *Phys Fluids* 2010;22:117102-1–117102-17.
- [2] Jones SF, Evans GM, Galvin KP. Bubble nucleation from gas cavities – a review. *Adv Colloid Interface Sci* 1999;80:27–50.
- [3] Apfel RE. The role of impurities in cavitation – threshold determination. *J Acoust Soc Am* 1970;48:1179–86.
- [4] Smith BL, Bruno TJ. Composition-explicit distillation curves of aviation fuel JP-8 and coal-based jet fuel. *Energy Fuels* 2007;21:2853–62.
- [5] Ritchie GD, Bekkedal MYV, Bobb AJ, Still KR. Biological and health effects of JP-8 exposure. Report no. TOXDET 01-01, Naval Health Research Center Detachment (Toxicology), Wright-Patterson Air Force Base, OH; 2001.
- [6] Mayfield HT. JP-8 composition and variability. Report no. AL/EQ-TR-1996-0006, Armstrong Laboratory, Environmental Research Division, Tyndall Air Force Base, FL; 1996.
- [7] Handbook of aviation fuel properties, 3rd ed., Coordinating Research Council, Inc.; 2004.
- [8] Edwards T, Maurice LQ. Surrogate mixtures to represent complex aviation and fuel rockets. *J Propul Power* 2001;17:461–6.
- [9] Violi S, Yan EG. Experimental formulation and kinetic model for JP-8 surrogate mixtures. *Combust Sci Technol* 2002;174:399–417.
- [10] Krieger IM, Mulholland GW, Dickey CS. Diffusion coefficients for gases in liquids from rates of solution of small bubbles. *J Phys Chem* 1967;71:1123–9.
- [11] Leighton JB. Pressure and diffusion-driven bubble growth on a static surface. MS thesis, University of Notre Dame, Notre Dame, IN; November 2006.
- [12] Dunn PF. Measurement and data analysis for engineering and science. 2nd ed. Boca Raton (FL): Taylor & Francis/CRC Press; 2010.
- [13] Mackay D, Shiu WY, Ma KC. Illustrated handbook of physical-chemical properties and environmental fate for organic chemicals. Volatile organic chemicals, vol. III. Ann Arbor (MI): Lewis Publishers; 1993.
- [14] JP-8 volatility study. Report no. IERA-RS-BR-SR-2001-0002, Southwest Research Institute, San Antonio, TX; 2001.
- [15] White FM. Fluid mechanics. 6th ed. New York (NY): McGraw-Hill; 2006.
- [16] Ran B, Katz J. The response of microscopic bubbles to sudden changes in ambient pressure. *J Fluid Mech* 1991;224:91–115.
- [17] Epstein PS, Plesset MS. On the stability of gas bubbles in liquid-gas solutions. *J Chem Phys* 1950;18:1505–9.
- [18] He J, Watson LT, Ramakrishnan N, Schafer CA, Verstak A, Jiang J, et al. Dynamic data structures for a direct search algorithm. *Comput Optim Appl* 2002;23:5–25.
- [19] Jones JR, Perttunen CD, Stuckman BE. Lipschitzian optimization without the Lipschitz constant. *J Optim Theory Appl* 1993;79:157–81.
- [20] Incropera FP, Dewitt DP. Fundamentals of heat and mass transfer. 5th ed. New York: John Wiley & Sons, Inc.; 2006.
- [21] Byrd RB, Stewart WE, Lightfoot EN. Transport phenomena. 2nd ed. New York: John Wiley & Sons, Inc.; 2002.
- [22] The installation restoration program toxicology guide, vol. 4, Oak Ridge National Laboratory, report no. A200512; 1989.
- [23] Mackay D, Shiu WY. A critical review of Henry's law constants for chemicals of environmental interest. *J Phys Chem Ref Data* 1981;10:1175–99.
- [24] Shimmiya Y, Yano T. Diffusion-controlled shrinkage and growth of an air bubble entrained in water and in wheat flour particles. *Agric Biol Chem* 1987;51:1935–40.
- [25] Green DW, Perry RH. Perry's chemical engineers' handbook. 8th ed. New York: McGraw-Hill; 2008.
- [26] Liebermann L. Air bubbles in water. *J Appl Phys* 1957;28:205–11.
- [27] Wise DL, Houghton G. The diffusion coefficients of ten slightly soluble gases in water at 10–60 °C. *Chem Eng Sci* 1966;21:999–1010.